Re-igniting the afterglow plasma column of an AC powered gliding arc discharge in atmospheric-pressure air

Kong, Chengdong; Gao, Jinlong; Zhu, Jiajian; Ehn, Andreas; Aldén, Marcus; Li, Zhongshan

Published in:
Applied Physics Letters

DOI:
10.1063/1.5041262

2018

Document Version:
Publisher's PDF, also known as Version of record

Applied Physics Letters

Re-igniting the afterglow plasma column of an AC powered gliding arc discharge in atmospheric-pressure air

Cite as: Appl. Phys. Lett. **112**, 264101 (2018); https://doi.org/10.1063/1.5041262
Submitted: 23 May 2018 • Accepted: 11 June 2018 • Published Online: 25 June 2018

Chengdong Kong, Jinlong Gao, Jiajian Zhu, et al.

Re-igniting the afterglow plasma column of an AC powered gliding arc discharge in atmospheric-pressure air

Chengdong Kong,[1] Jinlong Gao,[1] Jiajian Zhu,[1,2] Andreas Ehn,[1] Marcus Aldén,[1] and Zhongshan Li[1]
[1]*Division of Combustion Physics, Lund University, P.O. Box 118, S-221 00 Lund, Sweden*
[2]*Science and Technology on Scramjet Laboratory, National University of Defense Technology, Changsha 410073, China*

(Received 23 May 2018; accepted 11 June 2018; published online 25 June 2018)

The stability and re-ignition characteristics of the plasma column of an alternating current (AC) powered gliding arc discharge operating in atmospheric-pressure air were investigated for better plasma-mode controlling and optimized applications. By modulating the AC power supply and the air flow field, the states of afterglow plasma column were varied. When pulsating the AC power supply sequence, re-ignitions of the afterglow columns were introduced and their characteristics were studied using simultaneous high-speed photography and electrical measurements. Two re-ignition types were observed in the afterglow column with different decay times (the temporal separation of two sequential pulsed AC power trains). For a short decay time (<200 μs at 10 l/min air flow), the afterglow column can be recovered mildly without current spikes, which is called a glow re-ignition event. If the decay time is so long that the electric field strength becomes larger than 120 kV/m, the re-ignition event occurs with current spikes and bright emissions, which is called a spark re-ignition event. A quasi-equilibrium model is proposed to estimate the chemical compositions in the plasma column and to explain the observed phenomena. It infers that the chemical dissociation and ionization processes enhanced by vibrationally excited nitrogen molecules are dominating in the afterglow plasmas and thereby the electrons can survive a long time to keep the conductivity of the afterglow column, forming a glow re-ignition event. Whereas under large electric field strength (>120 kV/m), the electron impact ionization becomes dominant to trigger the spark re-ignition event. *Published by AIP Publishing*. https://doi.org/10.1063/1.5041262

Atmospheric-pressure air plasma discharges have been extensively used in the fields of material modification,[1,2] environmental remediation,[3] biomedical,[4,5] and combustion assistance[6] due to their easy handling and low costs. Usually, the non-thermal glow-type discharge is required to keep the chemical selectivity in these applications. However, glow discharges are difficult to sustain at atmospheric pressure due to the instabilities (e.g., the thermal instability and the thermionic emission of electrons from the cathode surface) which easily result in the glow-to-spark transitions.[7] Therefore, techniques based on using very short high voltage (HV) pulses[6] and ballasting the discharge with a current-limiting resistor[8] have been applied to prevent the transition of the reactive "cold" plasma to the thermal plasma. Recently, the gliding arc (GA) discharge has been recognized as a promising non-thermal plasma source for producing high operating power at atmospheric pressure.[9] In our previous studies, a self-sustained diffusive alternating current (AC) gliding arc (GA) with large volume and high power was reported.[9–14] This glow-type GA discharge was comprehensively diagnosed with various electrical and optical techniques. The conductive column of this GA discharge was contracted at atmospheric pressure to a filament with a diameter of around 1 mm,[11] and thus the electron number density can be estimated to be around 10^{19} m^{-3} using the following equation:

$$n_e = I/\left(\pi r_{arc}^2 e \mu_e E\right), \quad (1)$$

where n_e is the electron density, I is the electrical current, r_{arc} is the arc radius, e is the elemental charge, μ_e is the electron mobility, and E is the electric field strength. The translational temperature of the plasma column is below 2000 K, measured by the Rayleigh scattering method, but the vibrational temperature reaches as high as 5000 K and the electron temperature is around 1 eV.[13] Similar results have also been obtained in an annular-mode gliding arc discharge.[15] Therefore, the glow-type GA discharge belongs to non-thermal plasma type. Nevertheless, the performance of the glow-type GA discharge can be easily impacted by a turbulent flow.[12] Strong turbulence produces frequent glow-to-spark transitions. In order to gain more insight into this discharge and acquire detailed knowledge of the glow-to-spark transitions, experiments were designed to investigate the stability of the glow-type plasma columns and their re-ignition characteristics in the afterglow states. During experiment, the electron density and the electron temperature were controlled indirectly. The electron temperature, which is correlated to the reduced electric field strength, is varied by changing the jet flow rate. The electron density is varied by altering the decay time in the afterglow stage.

The details of the gliding arc discharge system have been described in our previous works.[10–12] Here, only a brief description is given. A schematic of the experimental setup is shown in Fig. 1. The system is operated in open air at atmospheric pressure. The gliding arc discharge is ignited at the narrowest gap between two diverging electrodes, which

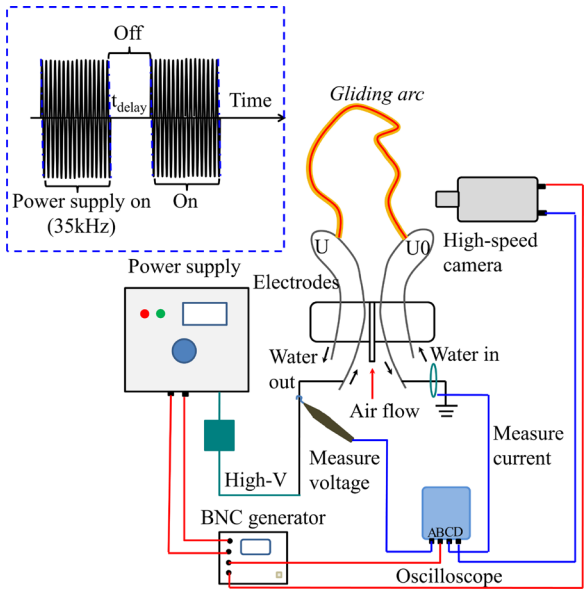

FIG. 1. Schematics of experimental setup.

are hollow stainless steel tubes with an outer diameter of 3 mm and internally water-cooled. The minimum gap between the two electrodes is around 5 mm. One of the electrodes is connected to a 35 kHz AC power supply (Generator 9030 E, SOFTAL Electronic GmbH), whereas the other electrode is grounded. The air flow is ejected through a 3-mm diameter hole between the two electrodes to push the generated plasma column upward, forming a gliding arc. The power supply has two modes: one is the continuous mode where the power supply works without interruption; the other is the burst mode where the power supply is modulated by a digital pulse generator to provide pulsed high voltage trains.

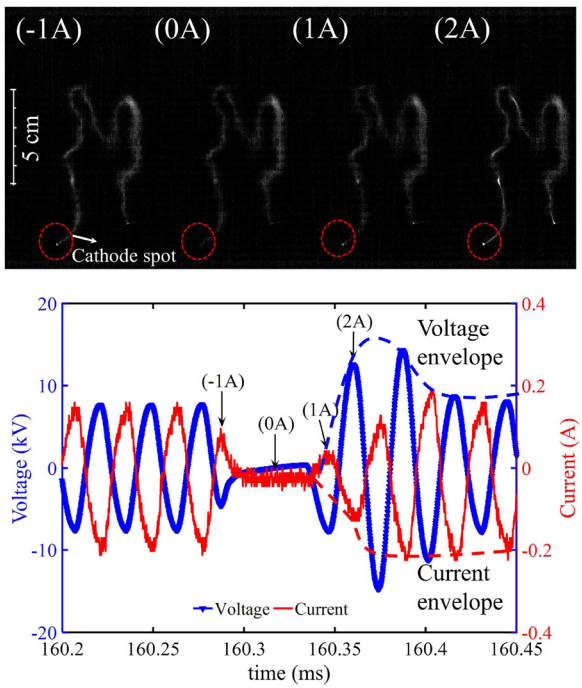

FIG. 2. Snapshots of the plasma column during the delay period (56 μs), together with the current-voltage waveforms at 10 l/min. The number in the images represents the sequence in the I-U curves. The phase of the current is inversely plotted.

In the experiment, the burst mode was chosen to control the afterglow state by varying the delay time between voltage bursts (t_{delay}), as illustrated in the inset of Fig. 1. A current monitor (Pearson Electronics) and a voltage probe (Tektronix P6015A) were used to measure the waveforms of the current and the voltage simultaneously. A high speed camera (HSC, Fastcam SA-Z, Photron) equipped with an objective lens (Micro-Nikkor UV 105 mm, f3.5) was synchronized with the discharge to capture the dynamics of the gliding arc column. Measurements were performed at a frame rate of 35 kHz with an exposure time of 15 μs. The current and voltage together with the HSC gate and the external trigger signals were simultaneously recorded using a four-channel oscilloscope (PicoScope 4424, PS) at a sample rate of 2 GHz. The synchronization between the current/voltage and the HSC was achieved through external triggering by a pulse generator (BNC 575).

By modulating the power supply to the burst mode, the re-ignition characteristics in the afterglow channel was detected. Phenomenologically, two re-ignition types have been observed, as demonstrated in Figs. 2 and 3, which show the typical emission of afterglow columns between the voltage bursts, together with the current and voltage waveforms. In order to show the current and voltage waveforms clearly, the phase of the current is inversely plotted. When the delay time between the voltage bursts (t_{delay}) is only 56 μs, the re-ignition of plasma column is mild (see Fig. 2). In Fig. 2(0A), when the power supply is switched off, the current and

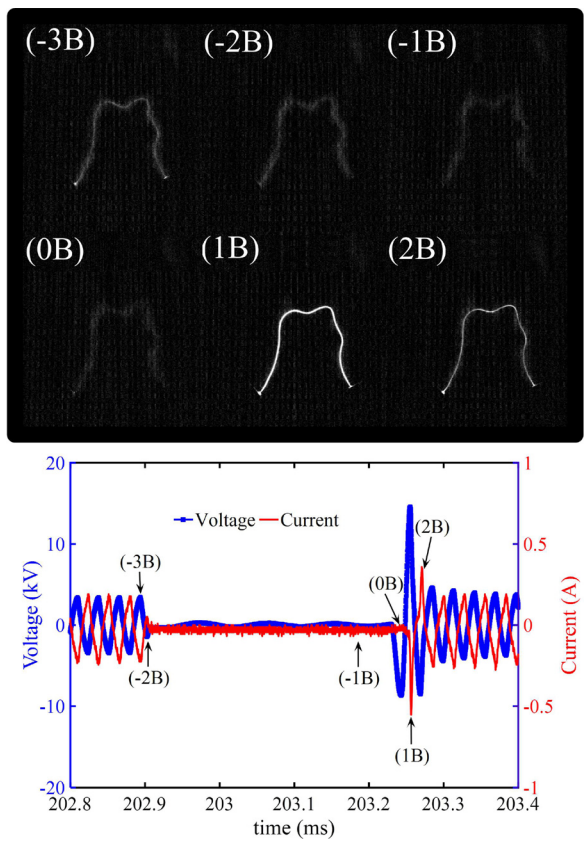

FIG. 3. Snapshots of the plasma column during the delay period (336 μs), together with the I-U curves at 10 l/min. The number in the images represents the sequence in the I-U curves. The phase of the current is inversely plotted.

voltage drop to zero fast, and the emission from the cathode spot disappears suddenly. But the luminance of the diffusive arc column changes slowly. When the power supply restarts, the current envelope increases continuously to a stable value and the voltage envelope experiences an increment first (overshooting) followed by a decay to a steady value. The cathode spot becomes bright when the power supply is switched on [see Fig. 2(1A)]. This mild re-ignition event can be called as a glow re-ignition event.

However, for the case with a long delay time of 336 μs, the emission of plasma column is gradually fading out during the delay period, but when the power supply restarts, the current and voltage spikes are shown up, together with the bright and uniform emission from the discharge channel, as demonstrated in Fig. 3. This uniform, bright, and thin arc channel [see Fig. 3(1B)] implies a strong ionization of the whole plasma column. This re-ignition event is quite different from that in Fig. 2 and is called as a spark re-ignition event. In fact, similar transient bright emission of the plasma column has been observed when the jet flow rate is so high that the mean electric field strength (E) in the plasma column reaches a threshold of around 120 kV/m.[12]

Figure 4 shows the mean electric field strength of re-ignition (E_{reig}) with respect to t_{delay} at a jet flow rate of 10 l/min. E_{reig} is the measured peak voltage divided by the gliding arc length during re-ignition of the plasma column. In the continuous mode of the power supply (i.e., $t_{delay} = 0$), the glow-type gliding arc could be sustained with an electric field strength of 34 kV/m. As t_{delay} increases, E_{reig} rises up linearly until reaching a critical value (ca. 120 kV/m). With a further increase in t_{delay}, the slope of the E_{reig}–t_{delay} curve changes to a smaller value. This change corresponds to the transition from the glow re-ignition event to the spark re-ignition event.

In order to clarify the underlying mechanisms of the glow re-ignition event and the glow-to-spark transitions, the afterglow states (including gas temperature and chemical compositions) modified with t_{delay} need to be explored. Actually, to mitigate the turbulent effect, the jet flow rate is set to 10 l/min. Such a flow rate ensures a laminar property of the flow around the plasma column. Under this laminar condition, the time scale of thermal diffusion is estimated to be around 20 ms, which is much larger than the delay time between voltage bursts ($t_{delay} < 0.5$ ms). Therefore, the translational gas temperature (T_g) can be assumed constant in the delay period. As for the chemical compositions, the decaying process of electronically excited OH* has been detected based upon the spectral emissions. It indicates OH* has a lifetime of hundreds of microseconds. The decaying electron density in the afterglow column is roughly estimated from the resistance of plasma column, which is the voltage divided by current. Figure 5, which shows the ratio of resistances after and before the burst delay with respect to the delay time, indicates that the resistance almost increases linearly with the delay time. It suggests a nearly linear decay of the electron number density within a time scale of two hundred microseconds.

To fully describe the chemical compositions, especially the electron density, in the afterglow plasma column, a quasi-equilibrium approximation model which assumes the chemical compositions of the afterglow plasma can be approximated by the chemical equilibrium compositions corresponding to an effective temperature is proposed. For this quasi-equilibrium approximation model, it is tricky to estimate the effective temperature. As we know, the glow-type plasma is non-thermal with quite different vibrational and translational temperatures.[13] In essence, the translational temperature (T_g) mainly impacts the collisional frequency between molecules while the vibrational temperature (T_v) can influence the chemical reactions during collisions. Therefore, if T_v is much larger than T_g, the vibrational temperature plays a dominant role in the dissociation reactions, and thus represent the chemical compositions better than the translational temperature. As a result, the vibrational temperature is chosen to assess the equilibrium chemical compositions. Using the CEA chemical equilibrium program,[16] with a presumed effective vibrational temperature of 4500 K, the calculated electron density is 2×10^{19} m^{-3}, which is close to the experimental value. Under this condition, the time scale of dissociative reactions in the air is of the order of 10 μs.[17] It is also estimated that the time scale of electron-ion recombination is on the order of 1 μs when the electron density is around 10^{19} m^{-3},[18] which is much smaller than the effective

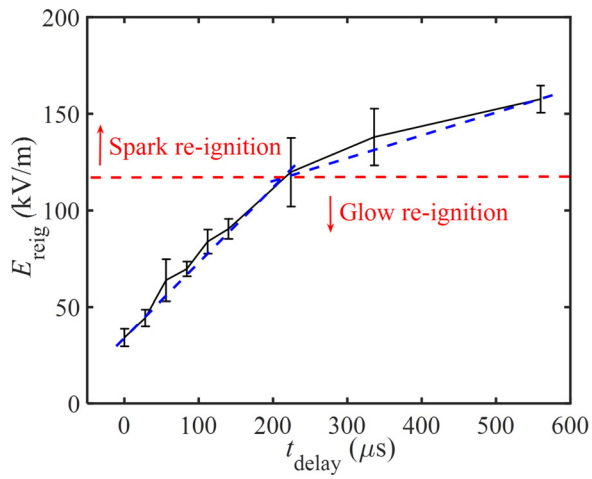

FIG. 4. Mean electric field strength of re-ignition (E_{reig}) with respect to the delay time between voltage bursts (t_{delay}).

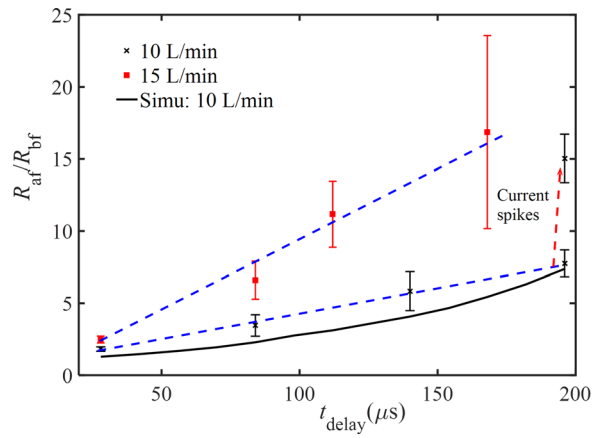

FIG. 5. Ratio of resistances after and before the burst delay (R_{af}/R_{bf}) with respect to the delay time (t_{delay}). The black solid line is a simulated result.

decay time in Fig. 5. To balance this fast recombination process, some ionization pathways must exist. The most possible ionization pathways during the decay process are associative/chemical ionizations between energetic atoms (such as $N + O => NO^+ + e$).[17] Since the diffusion process is relatively slow, having a time scale of 10 ms, the fast dissociative, recombination and ionization processes ensure a nearly local equilibrium state.

In the glow-type discharge, the input electric energy is first used to excite the nitrogen and later the gas is heated through the vibrational-translational (V-T) transition.[19] Therefore, the relaxation of vibrational temperature in the afterglow state can be described by Eq. (2), which represents the V-T relaxation rate of nitrogen.

$$d\varepsilon_V/dt = [\varepsilon_V - \varepsilon_V(T_g)]/\tau_{VT}, \tag{2}$$

$$\varepsilon_V(T) = E_{N2} \Big/ \left[\exp\left(\frac{E_{N2}}{T}\right) - 1\right], \tag{3}$$

where ε_V is the mean vibrational energy; τ_{VT} is the V-T relaxation time; and E_{N2} is the vibrational excitation level of N_2 (0.29 eV). Using the estimated decaying vibrational temperature, the decaying electron density can be calculated, as illustrated by black solid line in Fig. 5. The proposed model describes the slow decay process of electrons very well.

The experimental result also indicates that the turbulent flow impacts the decay rate of electron density greatly. As shown in Fig. 5, the slope of a 15 l/min case is larger than that of a 10 l/min case. This result is explained by the rapid decrement of the transport time scale as the flow rate increases. At a high flow rate, the gas temperature cannot be assumed constant during the delay period of voltage bursts. Instead, the temperature drops fast due to the strong turbulent mixing with surrounding cold gas. Therefore, the effective vibrational temperature and the electron density both decrease fast in the afterglow stage when the flow rate is high.

The mild recovery of glow-type plasma in the atmospheric air with short delay time (i.e., the glow re-ignition event) is naturally explained with the proposed model. After a short delay time, the electron density inside the plasma column is still high. When the power supply is switched on, the electrical energy is input through the residual electrons to balance the V-T relaxation. Consequently, the vibrational temperature stops dropping but increasing, along with the electron density growth. This process does not need the violent electron impact ionization, and thus, the current recovers without spikes. However, if the decay time is long, the electron density is quite low, and thus, the electric field strength can reach a value above the breakdown strength (~120 kV/m). Then, the electron-impact ionization occurs to cause the sudden brightening of plasma column and the current spikes.

In summary, the re-ignition characteristics of afterglow plasma column have been investigated by modulating the power supply and flow field. The results indicate two re-ignition types (i.e., the glow- and spark re-ignition events) with respect to the delay time between voltage bursts. For a short burst delay (<200 μs), the afterglow column can be recovered mildly without current spikes due to the chemical/associative ionizations enhanced by high vibrational temperatures. For a long burst delay, the re-ignition always accompanies current spikes and strong emissions due to the electron impact ionization under the large electric field strength (>120 kV/m). The glow-to-spark transition is essentially a transition from chemical/associative ionization to electron impact ionization here.

The work was financially supported by the Swedish Energy Agency, the Swedish Research Council, the Knut and Alice Wallenberg Foundation, and the European Research Council.

[1]Y. Kusano, S. Teodoru, F. Leipold, T. L. Andersen, B. F. Sorensen, N. Rozlosnik, and P. K. Michelsen, Surf. Coat. Technol. **202**, 5579–5582 (2008).
[2]Y. Kusano, B. F. Sorensen, T. L. Andersen, H. L. Toftegaard, F. Leipold, M. Salewski, Z. Sun, J. Zhu, Z. Li, and M. Alden, J. Phys. D: Appl. Phys. **46**, 135203 (2013).
[3]M. Magureanu, N. B. Mandache, and V. I. Parvulescu, Water Res. **81**, 124 (2015).
[4]H. Tanaka, M. Mizuno, K. Ishikawa, H. Kondo, K. Takeda, H. Hashizume, K. Nakamura, F. Utsumi, H. Kajiyama, and H. Kano, Clin. Plasma Med. **3**, 72 (2015).
[5]D. W. Kim, T. J. Park, S. J. Jang, S. J. You, and W. Y. Oh, Appl. Phys. Lett. **109**, 233701 (2016).
[6]W. Kim, M. G. Mungal, and M. A. Cappelli, Appl. Phys. Lett. **92**, 051503 (2008).
[7]L. Prevosto, H. Kelly, B. Mancinelli, J. C. Chamorro, and E. Cejas, Phys. Plasmas **22**, 023504 (2015).
[8]M. Janda, Z. Machala, L. Dvonč, D. Lacoste, and C. Laux, J. Phys. D: Appl. Phys. **48**, 035201 (2015).
[9]J. Zhu, J. Gao, Z. Li, A. Ehn, and M. Alden, Appl. Phys. Lett. **105**, 234102 (2014).
[10]Z. Sun, J. Zhu, Z. Li, M. Alden, F. Leipold, M. Salewski, and Y. Kusano, Opt. Express **21**, 6028–6044 (2013).
[11]J. Zhu, Z. Sun, Z. Li, A. Ehn, M. Alden, M. Salewski, F. Leipold, and Y. Kusano, J. Phys. D: Appl. Phys. **47**, 295203 (2014).
[12]J. Zhu, J. Gao, A. Ehn, M. Alden, A. Larsson, Y. Kusano, and Z. Li, Phys. Plasmas **24**, 013514 (2017).
[13]J. Zhu, A. Ehn, J. Gao, C. Kong, M. Alden, M. Salewski, F. Leipold, Y. Kusano, and Z. Li, Opt. Express **25**, 20243–20257 (2017).
[14]C. Kong, J. Gao, J. Zhu, A. Ehn, M. Alden, and Z. Li, Phys. Plasmas **24**, 093515 (2017).
[15]T. Zhao, J. Liu, X. Li, J. Liu, Y. Song, Y. Xu, and A. Zhu, Phys. Plasmas **21**, 053507 (2014).
[16]S. Gordon and B. J. McBride, "Computer program for calculation of complex chemical equilibrium compositions and applications," NASA Reference Publication Report No. 1311, 1996.
[17]K. H. Becker, U. Kogelschatz, K. H. Schoenbach, and R. J. Barker, *Non-Equilibrium Air Plasmas at Atmospheric Pressure* (IOP Publishing, Bristol, 2005).
[18]M. Capitelli, C. M. Ferreira, B. F. Gordiets, and A. I. Osipov, *Plasma Kinetics in Atmospheric Gases* (Springer, Berlin, 2000).
[19]N. A. Popov, Plasma Phys. Rep. **27**, 886–896 (2001).